Available online at www.sciencedirect.com
SCIENCE DIRECT
Biosensors and Bioelectronics 21 (2006) 1746–1752
BIOSENSORS & BIOELECTRONICS
www.elsevier.com/locate/bios

dc-Sheet resistance as sensitive monitoring tool of protein immobilization on thin metal films

H. Neff [a,d,*], T. Beeby [b], A.M.N. Lima [a], M. Borre [c,d], C. Thirstrup [d], W. Zong [d], L.A.L. de Almeida [e]

[a] *Universidade Federal de Campina Grande, Department of Electrical Engineering, Campina Grande, Brazil*
[b] *Danish Technological University, Lyngby, Denmark*
[c] *Biodet A/S, Copenhavn, Denmark*
[d] *VIR Biosensor, Taastrup, Denmark*
[e] *Universidade Federal da Bahia, Department of Electrical Engineering, Salvador, Brazil*

Received 2 July 2005; received in revised form 20 August 2005; accepted 22 August 2005
Available online 26 October 2005

Abstract

The suitability of high resolution, in situ dc-sheet resistance monitoring (SRM) as a simplified and reliable sensing technique towards detection and tracking of protein immobilization has been explored. Non-specific adsorption of bovine serum albumin (BSA) onto a very thin gold film, acting as the sensing resistor, has been employed as a model system. For comparison, the novel sensing method was combined with surface plasmon resonance (SPR) spectroscopy, using the same flow cell and sensing surface. Two different, well known adsorption states, involving a composite layer of irreversibly and reversibly bound BSA, were clearly resolved by both methods. Clearly structured, pronounced and fully reproducible film resistance modulations have been resolved in the associated SRM data. The transition from reversibly bound BSA to the diluted protein phase is associated with an unusually large decrease in the dc-sheet resistance. The observed resistance modulation magnitude for an adsorbed BSA monolayer corresponds to approximately 1%, and up to 100 mΩ at a 10 Ω sensing resistor. The sheet resistance of irreversibly bound BSA was determined to 0.24 kΩ/cm^2, and the associated specific resistivity estimated to 1–2 × 10^4 Ω cm.

Keywords: Sheet resistance; Biosensor; Thin film detection; Protein adsorption; Immobilization; Hopping conduction

1. Introduction

The availability of easy to integrate, reliable and reproducible detection methods of immobilized biochemical films on surfaces, combined with easy to interpret output signals is a crucial issue towards realization of low cost biosensors, particularly in connection with future lab-on-chip technologies. A large number of technically demanding sensing principles has been developed in the past few years, to explore the immobilization properties of proteins and other biotic material on solid surfaces (Rogers and Mulchandani, 1998). The non-specific adsorption characteristic of human serum albumin (HSA) and bovine serum albumin (BSA) on bare and modified thin gold and silver films has been investigated by means of surface plasmon resonance (Silin et al., 1997), quartz microbalance recordings (Mao et al., 2001) and by cyclic voltammetry (Moulton et al., 2003). Wee et al. (2005) reported recently about a novel, label free electrical detection method for disease marker proteins, employing piezoresistive micro-cantilevers.

Albumin proteins commonly reveal an anisotropic shape, and their orientation on hydrophilic surfaces is known to vary with surface coverage (Edmiston et al., 1997; Koutsoukos et al., 1982). BSA features a more triangular, heart like shape, with approximately 8 nm side lengths and 3 nm depths (Norde and Giacomelli, 2000). Both BSA and HSA represent important model proteins for biosensing applications. At present, there is only very limited information available, regarding the physical connection between adsorption/desorption characteristics, structure and electrical/electronic transport properties of very thin protein films, exhibiting thickness at the monolayer range. Highly controversial charge carrier transport mechanisms have

* Corresponding author.
E-mail address: hneff@get2net.dk (H. Neff).

0956-5663/$ – see front matter © 2005 Elsevier B.V. All rights reserved.
doi:10.1016/j.bios.2005.08.009

been reported for selected bio-electronic materials as mentioned in the following.

Quasi semi-conducting charge carrier transport has been observed for dried-out, oxygen hole doped DNA (Lee et al., 2002). Nearly metallic conduction of specific globular proteins, like cytochrome *c* (CC) and BSA in the dried-out, de-natured state has been claimed recently (Deb, 1999).

In contrast, earlier research work on charge transport properties of bulk samples of BSA provided clear evidence for proton hopping as the most likely protein conduction mechanism. Charge carrier hopping, in connection with presence of surface bound vicinal water layers, also has been identified as a dominating carrier transport mechanism in oriented DNA films (Kutnjak et al., 2005). De-naturation associated with partial loss of the hydration shell also persists for protein adsorption on solids in aqueous solution, primarily induced by the pronounced interaction of the carboxylate group with the bare metal surface (Loesche, 1997).

In this work, preliminary research results on biochemical sensing properties of in situ (in-plane) dc-sheet resistance measurements are reported. BSA has been selected, since it can be used as a reference biomaterial, and the unspecific binding of HSA and BSA onto solid surfaces is well known (Moulton et al., 2003). BSA immobilization displays two different binding states, denoted as reversible and irreversible adsorption, and reveals pronounced differences between both kinetic binding constants (Kurrat et al., 1997).

dc-Resistance measurements are considered as easy to perform, routine electrical characterization methods. Incident radiation from the simultaneously operated SPR set-up does not significantly affect the SRM output signal. Commercial instrumentation, allowing for high-precision resistance recordings, is readily available at attractive cost and performance, combined with an easy readable electrical output signal. The presented detection tool offers a potential alternative for exploitation of the physical properties of immobilized proteins and other biotic material, eventually providing addition and complementary information to existing sensing methods.

2. Experimental

2.1. Materials

An optically transparent, electrically isolating plastic chip made from TOPAS material has been employed, where an electrical 4-point resistance measurement circuit was integrated with an optical SPR monitoring set-up in the Kretschmann configuration. Four separated contact areas for biasing current and parallel voltage read-out terminals have been formed on the chip. Connection to thin copper wires was established, using silver paint contacts. To maintain stable contact resistance, and suppress initially appearing drift effects during the measurements, a 12 h stabilization period was required after deposition of the silver paint. The sensing resistor was formed by a semi-transparent gold film at thickness of approximately 40 nm. It comprises a 1 mm wide and 10 mm long stripe in the center of the flow cell, accounting for a plain gold film sheet resistance value of about 10 Ω at ambient temperature. The thin film metal stripe was simultaneously employed as the SPR sensing spot. Active temperature control of flow cell and analyte temperature to <0.1 °C accuracy by a Peltier element has been used in the experiments.

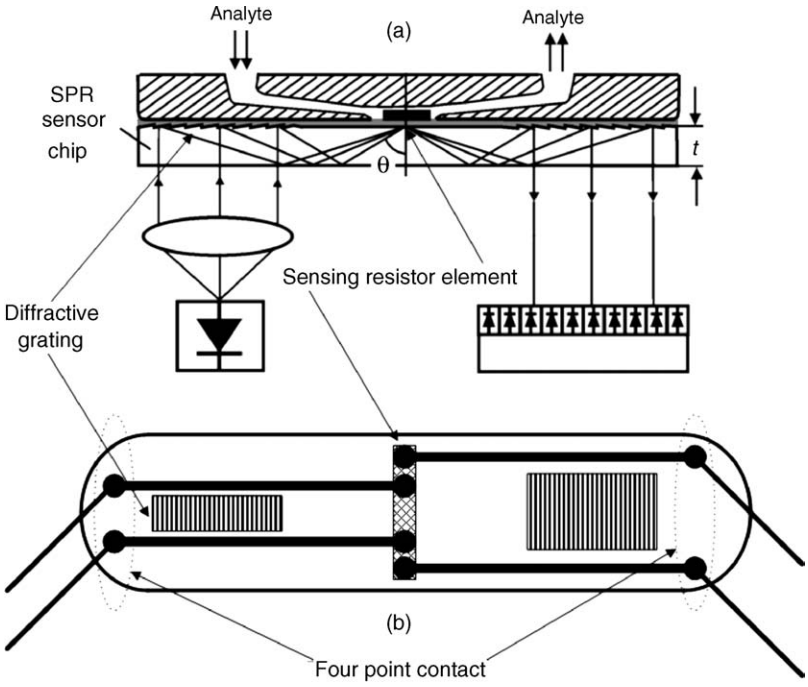

Fig. 1. (a and b) Upper cross-sectional view of the experimental set-up in (a) using a modified SPR optical chip for internal beam forming/guiding. The 4-point contact arrangement, illustrated (b) use gold coverage from the grating couplers, structured into the chip surface, to minimize contact resistance. Not shown are attached HP multimeter, and connected SPR data processing units.

The upper view of Fig. 1 illustrates a cross-sectional sketch of the experimental arrangement, employing a planar optical chip that allowed for combined surface plasmon resonance and sheet resistance sensing. The novel optical chip technology for surface plasmon sensing has been outlined in detail recently (Thirstrup et al., 2004; Neff et al., in press). The lower top view image in Fig. 1b illustrates the geometric arrangement of electrical contact areas, required to establish 4-point resistance readings.

2.2. Methods

All solutions used for this investigation were degassed by Argon bubbling, prepared from de-ionized Millipore filtered water at >1 MΩ resistance, and analytical grade chemicals. A peristaltic pump has been employed, at an analyte flow at a rate of 115 μL/min. The HP34401A digital multimeter in connection with associated data handling software has been used for the electrical measurements, allowing for μΩ resistance resolution over an integration period of 2 s. Initially, unwanted adsorbates present on the sensing gold surface were removed in situ by flow of 0.1 M NaOH solution through the flow cell for 1 h, which also removed possible contaminations from the inner surface of the Teflon tubes. The unspecific immobilization of BSA on a plain gold surface involved a four-step protocol I–IV:

I. *Surface cleaning*: The gold surface was cleaned and restored by 3 min injection of a 0.1 M NaClO solution, acting as a strongly oxidizing reagent. This treatment effectively removes possible traces of organic contaminations, including earlier immobilized biofilm from the gold surface, leaving a clean hydrophilic metal surface.
II. *Buffer rinse*: Removal of the NaClO solution from the flow cell by injection of an aqueous buffer for 3 min, containing a solution of 0.1 M MES in 0.05 M NaAc (MES: 2-morpholino-ethan-sulphonic acid: $C_6H_{12}NNaO_4S$), to stabilize the pH value at 6.5.
III. *Protein adsorption*: Injection of the same solution, containing 1000 μg/mL BSA over the bare gold surface for 3 min, to establish unspecific immobilization of the protein onto the gold surface.
IV. *Buffer reflow*: Reflow of plain buffer solution for 3 min over the BSA covered surface, to remove reversibly, weakly bound protein material from the deposited BSA monolayer film, via convective diffusion into the solution phase.
V. Back to surface cleaning step I.

3. Results

During all steps I–IV, both dc-sheet resistance and SPR response have been monitored simultaneously. Fig. 2 compares the principal output signal features of both sensing methods. The data illustrate the effect of solution/flow cell temperature on film resistance of a plain gold film resistor, and the associated refractive index variation, obtained from the SPR measurement, in response to an approximately 10 °C/5 °C temperature variation of an injected aqueous solution. Both sensing methods reveal opposite signal variations with temperature, due to the positive

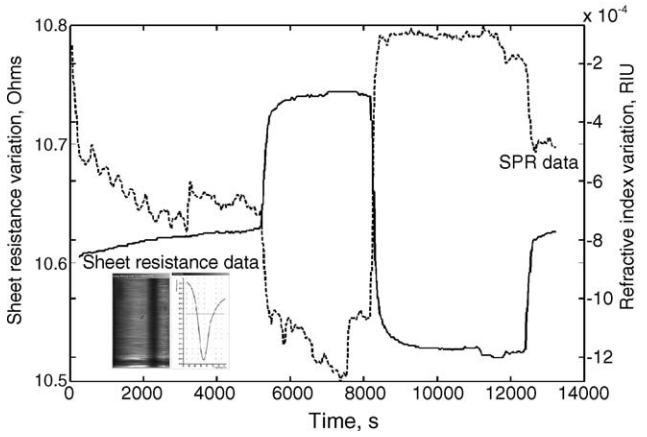

Fig. 2. Simultaneous response of SPR and SRM recordings of a plain gold film to temperature variations of 10 and 5 °C, respectively, of an injected aqueous MES-solution. Initial periodic fluctuations in the SPR signal result from influence of air bubbles, not affecting the SRM data. The inset illustrates the optically recorded SPR absorption line, and associated reflectance minimum as a function of incident angle.

resistance temperature coefficient (TCR) of the gold film at a magnitude of +0.35%/°C, and a negative TCR of water at a level of -1.2×10^{-4} RIU/°C; RIU stands for refractive index units. The data also depict and compare the achievable output signal fluctuation levels of both sensing methods, employing similar integration times. It is evident that the SRM output signal reveals a substantially reduced noise level. Initial periodic modulations in the SPR signal most likely originate from influence of air bubbles, in combination with the operation of the peristaltic pump. It is interesting to note that the presence of air bubbles does not appear in, and detoriate the SRM output signal. The inset depicts both, an image of the sharp SPR absorption line, generated by the optical chip and received at the optical receiver, and the associated SPR-minimum as a function of incident angle, as calculated from the digitized image.

Fig. 3a and b illustrates the principal features of both sensing methods, to detect/monitor BSA protein adsorption. The SPR response, recorded during the immobilization procedure, displays the variation of the (effective) film refractive index as a function of time. The SRM response provides the variation of the recorded resistance, given in Ohms. The individual steps I–IV assigned to the BSA immobilization protocol are indicated in the figure. The cleaning procedure of the gold surface, using the oxidizing solution in step I, is accompanied in the SPR signal by a rapid increase of the refractive index and stabilization at a fixed value of $\Delta n = 1.24 \times 10^{-2}$. It originates from the change of the RIU of the bulk solution. The SRM-signal shows an initially rapid variation, followed by a rather slow and steady increase in resistance, without appearance of signal saturation. Injection of the buffer solution in step II leads to a decrease in the RIU variation and rapid stabilization, but only to a relatively small decrease of the film resistance in the SRM. Admission of the BSA containing solution during step III results in a steady increase of the RIU and signal saturation after approximately 3 min, at a level of $\Delta n = 6.5 \times 10^{-3}$, due to immobilization of

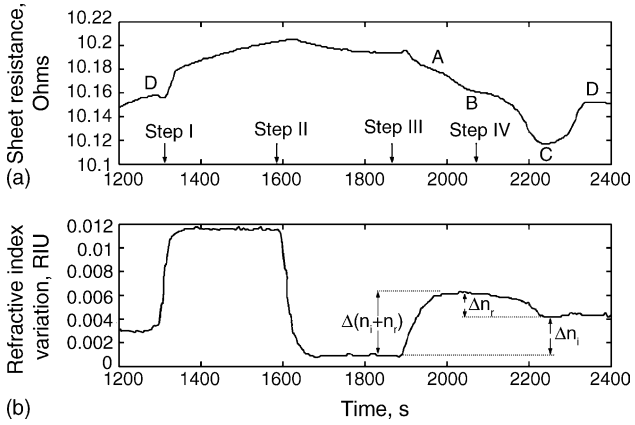

Fig. 3. (a and b) Comparison of surface plasmon resonance and sheet resistance data, displayed as function of time, under conditions of BSA protein immobilization. Steps I–IV and associated injections of solutions into the flow cell are indicated. Features: (A) coverage dependent surface re-orientation; (B) formation of re-hydrated network of reversibly bound BSA molecules; (C) removal of loosely bound proteins; (D) irreversibly bound stable BSA monolayer formation (denatured).

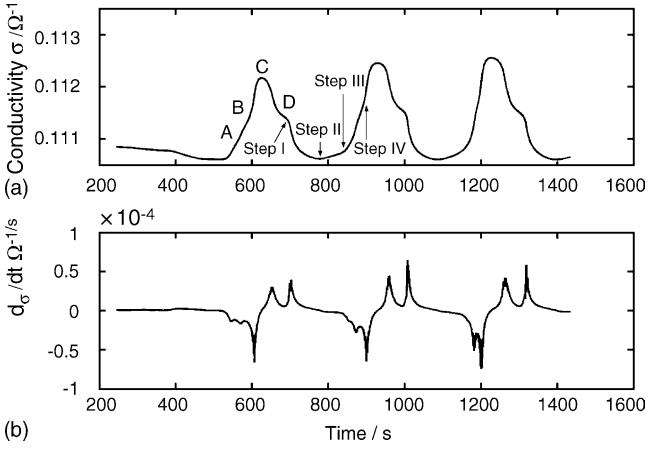

Fig. 4. (a and b) Reproducibility of SRM measurements, executed by three consecutive runs. Originally recorded dc-sheet resistance has been replaced by dc-sheet conductivity σ, plotted as a function of time. Data were recorded in absence of illumination from the SPR light source. Steps I–IV and features A–D are indicated in the figure. (b) It shows computed first derivative $d\sigma/dt$, as a function of time.

BSA molecules onto the gold surface. SPR signal evolution and saturation are determined by the kinetics, and associated affinity constants of BSA film growth via protein out-diffusion from the bulk analyte solution onto the bare metal surface. In contrast, the SRM-signal variation reveals a steady decrease in resistance, reaching a total magnitude of approximately 0.1 Ω at the minimum value. Clearly structured and reproducible variations in signal slopes are marked as A, B, C and D in the figure.

Feature “A” indicates a weak shoulder, which is approximately correlated with the onset of signal saturation in the SPR signal. “B” indicates onset of signal saturation in the SRM-signal. It is correlated with step IV, applied to remove the fraction of reversibly, i.e., weakly bound BSA proteins, achieved by re-injection and flow of plain buffer solution over the initially adsorbed BSA film. It manifests itself in the SPR signal as a slow steady decrease towards a stable value of $\Delta n = 3.8 \times 10^{-3}$ RIU, indicating the final presence of a stable, irreversibly bound BSA layer onto the plain gold film. The associated SRM-signal variation, related to step IV, reveals a surprisingly structured characteristics.

Absence of clear film growth saturation behaviour, as appears in the SPR data, but a further rapid decrease of total film resistance and presence of a pronounced minimum and signal swing, marked by arrow “C”. Eventually, feature “D” denotes final SRM-signal recovery, where a stable resistance variation value of approximately 43 mΩ with respect to the film resistance after applying step II is reached. At this level, all reversibly bound BSA proteins are removed, and a final layer of irreversibly bound BSA on the gold surface is left over.

However, SPR signal saturation of irreversibly bound BSA appears earlier, being correlated with the appearance of the SRM minimum. The resistance of the final irreversibly bound, and most likely monomolecular BSA layer at feature “D” is 2407 Ω, or 0.24 kΩ/cm^2 sheet resistance. It is calculated by assuming a single second protein conduction channel, shunted with the plain gold film beneath. Assuming a film thickness of the irreversibly bound BSA molecules of 5–8 nm, their estimated (specific) dc-resistivity can be placed within the range of $1–2 \times 10^4$ Ω cm. The total resistance variation upon adsorption of the composite BSA film at feature “C” is 1.34 kΩ.

Fig. 4a illustrates the signal quality and reproduciblity of the sheet resistance sensing method. Three consecutive runs are depicted, all of them including steps I–IV, as indicated in the figure. The present set of data has been gained in absence of illumination from the SPR light source, revealing that photo-induced resistance variations are virtually absent. The measurements have been performed on a second sample, exhibiting a slightly lower plain gold film resistance. Plotted here is the variation of $(1 - R_S)$ as a function of time. This quantity is related to the sheet conductivity σ_S, since reformulation yields the product $R_S\ (\sigma_S - 1)$. It approximately scales with the SPR signal. The quality of the recorded signal is illustrated in Fig. 4b, where the differentiated signal $d(1 - R_S)/dt$ is plotted as a function of time. This set of data reveals a pronounced and reproducible structure, with negative values corresponding to protein immobilization (step III) of the primary BSA monolayer, positive slope values originate from the surface cleaning and washing steps (steps II and IV).

4. Discussion

A full identification of the origin of the distinct dc-sheet resistance modulations observed for monomolecular BSA films on gold is a difficult issue, presently not allowing for quantitative data analysis. For qualitative interpretation, we adopt the albumin adsorption scheme the earlier published layer model (Kurrat et al., 1997). There, a three layer model has been suggested. It is composed of a primary layer of reversibly and irreversibly attached albumin molecules to the solid sorbent surface, a second molecular layer directly above, featuring preferably homomolecular binding mechanisms, and a third layer of convectively diffusing molecules, extending into the diffusion

boundary layer. The primary features of dc-sheet resistance variations are attributed to three effects.

Firstly, shunting of the gold film with a conducting primary protein layer composed of reversibly and irreversibly bound BSA. Contact resistance values for albumins as low as 0.5 Ω/in.^{2} under bias current of 1 mA have been reported (Deb, 1999). These findings support formation of a shunted conduction channel of the protein adlayer with the supporting gold film beneath.

Secondly, in the most simple model with increasing BSA film coverage, and improved intermolecular connectivity, film resistance should approximately linear decrease in the primary layer, as is observed by experiment in the initial phase of step III.

Thirdly, structural protein layer rearrangements and relaxation, including conformational transformations in the first layer. We tentatively attribute feature "A" to appearance of structural reorganization/relaxation within the protein based primary conduction channel, shunted with the underlying thin gold film. Coverage dependent variations of the vertical and horizontal orientation of HSA molecules have been reported earlier (Moulton et al., 2003), resulting in different protein surface concentrations of 6.85 and 1.96 mg m^{-2}, respectively. Thus, an increase in the orientation dependent BSA surface concentration also would account for a decrease of film resistance.

Feature "B" in the SRM data indicates onset of signal saturation, which appears in the SPR data somewhat earlier. It also correlates with the admission of plain buffer solution, by applying step IV. As mentioned before, the weakly, reversibly bound BSA molecules, contained in the primary layer, are removed by dilution and diffusion into the adjacent plain buffer solution. This is clearly resolved in the SPR data of Fig. 2. $\Delta(n_i + n_r)$ decreases by the amount Δn_r from its stable value in step III to Δn_i, indicating that the nominal film thickness decreases to the level of the irreversibly adsorbed BSA molecules (under action of step IV), where the lower constant refractive index value Δn_i is maintained.

Ultimately, thinner BSA film thickness should lead to an increase in the dc-sheet resistance. However, SRM data indicate a pronounced further decrease in film resistance in the transition section between "B" and the resistance minimum "C". The expected increase in BSA film resistance, where all reversibly bound BSA molecules are removed from the gold surface, appears slightly delayed in the SRM, denoted as feature "D".

To resolve the apparent contradiction between SRM and SPR data at this point, specific electrical protein properties, i.e., a substantially higher conductivity must be assigned to the reversibly bound, but already mobile BSA molecules. This phenomenon has not been observed before, and is attributed to increased hydration of BSA molecules in the diluted state. The physical origin of the observed effect can be related to the results of earlier research work of Gascoyne et al. (1981) on identifying the elemental charge transport mechanism in proteins. Dielectric measurements over a broad frequency span that include quasi dc-conductivity recordings as a function of hydration rate have been performed for bulk BSA samples. The dominant influence of water content and protein hydration, respectively, on electrical properties is illustrated in the rescaled Fig. 5, where the dc-resistance is plotted as a function of protein hydration. It should be noted that data were taken and derived from Fig. 3 of the original publication of Gascoyne et al. (1981) which illustrates the dc-conductivity of BSA as a function of molecular hydration. The initially de-natured, dehydrated BSA molecules reveal a rather high resistance, which steadily decreases with increasing hydration rate from 6×10^4 to 2×10^1 Ω cm at a hydration rate of 20%. The strong effect of vicinal water on the molecular conductivity invokes long and short range proton hopping as the dominant and ionic type conduction mechanism in proteins.

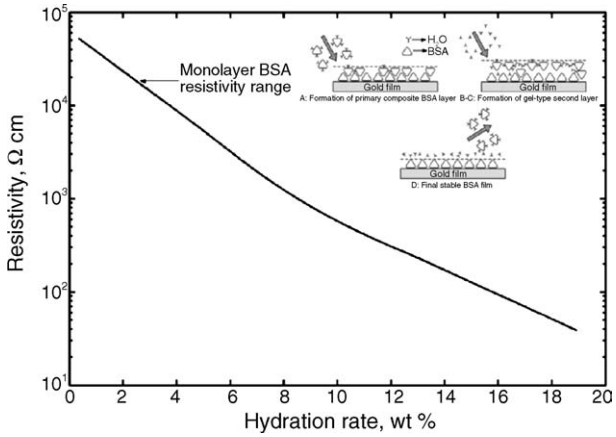

Fig. 5. Rescaled resistivity of BSA bulk material, plotted as function of hydration rate, with original dc-conductivity data set taken from literature. Arrow denotes experimentally determined resistivity range of monomolecular BSA film, irreversibly attached onto gold surface. The inset illustrates schematically the relevant adsorption/desorption features and conducting layer system of BSA on a thin gold film.

Here, we adopt this concept to account for the decreasing dc-sheet resistance, observed under specific action of step IV. The schematic illustrations provided in the inset of Fig. 5 illustrate the processes involved.

It is important to note that the assumption of forming a gel-type layer of re-hydrated BSA molecules within the transition region B → C is not in conflict with the SPR data, revealing a steady unstructured decreasing refractive index variation, upon application of step IV. Dense proteins reveal an absolute RI-value around 1.35–1.5, largely determined and approximately inversely scaling with their densities and molar weights (Vörös, 2004). It is reasonable to assume that with increasing protein hydration and dilution during step IV, the refractive index in the gel-type layer decreases towards the value of water (n: 1.333). This property would explain the observed lower RI value, taken from the related SPR signal.

Further support for the presence of a second shunted conduction channel of a re-hydrated BSA surface layer provides comparison of their specific resistivities. As mentioned before, for bulk BSA material in Fig. 5a value of 1×10^4 Ω cm has been determined experimentally at low hydration rates (Gascoyne et al., 1981). This value compares well with the estimated specific resisitivity of irreversibly adsorbed BSA on gold of 1–2 $\times 10^4$ Ω cm in this work.

It finally should be mentioned that other processes are invoked, affecting resistance of the plain gold film, but commonly shall lead to an increase in resistance.

Reduction of the mean free path and mobility of conduction electrons in the plain goldfilm, caused by scattering on surface inhomogenities, in combination with adsorption induced film surface relaxation and recrystallization processes. This effect most likely appears under action of step I, where an oxidizing cleaning solution is admitted to the gold surface.

It is interesting to note that the interaction of the hypochlorite solution with the plain gold surface when monitored with the SPR-spectrometer solely leads to an initially fast increase in the refractive index, but remains unchanged during persistent exposure of the metal surface to the solution. The refractive index variation here simply displays the higher bulk refractive index of the oxidizing hypochlorite solution.

Surprisingly, the associated sheet resistance variation, due to action of step I appears much more pronounced. The initial sharp increase in the SRM most likely originates from removal of the residual monolayer of irreversibly bound BSA molecules, attached to the gold surface at the previous cycle. The following slow, persistent increase in the SRM-signal most likely results from increased specific adsorption of Cl-ions and/or free chlorine from the oxidizing solution onto the gold surface. The adsorption level is near the monolayer range, possibly also associated with increased surface roughening. Both effects account for stronger surface scattering of free electrons within the gold film, and thus create an increasing film resistance. It is known from electrochemical studies in aqueous solution that halides reveal specific adsorption on noble metal surfaces (Hubbard, 1988).

Two important conclusions can be drawn from the above mentioned observations: Firstly, the apparent insensitivity of the SPR sensing method against variations of surface morphology is a clear indication of the exceptional surface sensitivity of the SRM-probing technique, being superior over the SPR method. Secondly, the (high frequency) metal dielectric function, probed by the SPR method, appears insensitive to morphological modifications at or near the metal surface.

A further possibility to increase film resistance can be attributed to a minor, persistent increase gold film temperature, induced by the surface plasmon decay itself. Approximately 10% of the incident radiation couple into the resonant surface plasmon excitation. Due to plasmon-phonon coupling, the absorbed radiation at a level of 5–10 μW accounts for minor film heating, causing an increase of film resistance. We estimate the temperature change to about $10^{-2}\,^{\circ}$C, corresponding to approximately $10^{-5}\,\Omega$, respectively.

It is interesting to note that structural biofilm variations have yet not been resolved neither in the present, or other reported SPR measurements, quartz micro balance, nor by electrochemical investigations, employing voltammetry and impedance measurements. As mentioned earlier, the SPR signal is determined by the high-frequency dielectric constants pertaining to the interfacial region, that are insensitive to the microscopic features and modifications in metal or adsorbed film morphology. The same conclusion would hold for cyclic voltammetric measurements.

We attribute the unexpected, exceptional surface sensitivity of the SRM sensing principle, when compared to other mentioned interfacial sensing methods, primarily to a geometry effect, pertaining to a physical system of reduced dimensionality. The sheet resistance signal results from directed, in-plane carrier transport, preferably along the interface between solid and liquid phases. Under these circumstances, elastic carrier scattering on surface/interface inhomogenities would add up over macroscopic distances.

It is not known whether protein multilayer arrangements, involving functionalized sensing surfaces on bases of self assembled monolayers, avidin, globular proteins and others, can be resolved by SRM. Whether the SRM technique is fully suited to monitor antigen–antibody interactions thus requires further investigations.

An experimental set-up, to evaluate the SRM instrumental performance for detection of immunological reactions is presently under preparation. Further improvements of the SRM sensing method should be achievable by reducing the geometric size of the sensing elements, thus allowing the realization of 1 or 2 dim resistor array arrangements. Using established microstructuring techniques, individual resistive sensor pixel areas down to 100 μm^2 should be feasible, employing a meandering sensing resistor structure at small line width around 1 μm.

5. Conclusion

The sensing capability of dc-sheet resistance measurements towards detection of protein immobilization on thin metal films has been demonstrated. Comparison with literature data suggests hopping conduction as the most likely conduction mechanism in adsorbed BSA films. The data clearly indicate, within a limited time span, the presence and formation of an interconnected diluted BSA film, formed by re-hydration of reversibly bound BSA molecules. The SRM method displays exceptional sensitivity to surface modifications, not resolvable by SPR sensing. Electrically, BSA growth induced sheet resistance modulations can be treated as build-up of primary and secondary protein conduction channels, shunted to the thin gold film beneath. BSA film growth correlates with a decrease in total film resistance at a magnitude of $43 \times 10^{-3}\,\Omega$/ML, corresponding to $0.24\,k\Omega/cm^2$ sheet resistance of the shunted, irreversibly bound protein monolayer. The present findings reveal that the SRM sensing approach may provide an alternative to SPR, quartz microbalance and electrochemical impedance sensing techniques. To achieve further improvements in sensitivity, it is beneficial to increase the resistance of the underlying gold film, towards the resistance level of the protein film. This can be achieved by both, reducing the gold film thickness, and increase the resistor length applying appropriate microstructuring techniques.

References

Deb, K.K., 1999. Update: a protein micro bolometer for focal plane arrays. Mater. Res. Innovation 3, 66–69.

Edmiston, P.L., Lee, J.E., Cheng, S.S., Saavedra, S.S., 1997. Molecular orientation distributions in protein films: cytochrome c adsorbed

to substrates of variable surface chemistry. J. Am. Chem. Soc. 119, 560–570.

Gascoyne, P.R.C., Pethig, R., Szent-Gyoergyi, A., 1981. Water structure dependent charge transport in proteins. Proc. Natl. Acad. Sci. USA 78, 261–265.

Hubbard, A.T., 1988. Electrochemistry at well characterized surfaces. Chem. Rev. 88, 633–656.

Koutsoukos, P., Mumme-Young, C., Norde, W., Lyklema, J., 1982. Effect of the nature of the substrate on the adsorption of human-plasma albumin. Colloids Surf. 5, 93–104.

Kurrat, R., Prenosil, J.E., Ramsden, J.J., 1997. Kinetics of human and bovine serum albumin adsorption at silica-titania surfaces. J. Colloid Interface Sci. 185, 1–8.

Kutnjak, Z., Lahajnar, G., Filipic, C., Podgornik, R., Nordenskjoeld, L., Korolev, N., Rupprecht, A., 2005. Electrical conduction in macroscopically oriented deoxyribonucleic and hyaluronic acid samples. Phys. Rev. E 71, 41901.

Lee, H.Y., Tanaka, H., Otsuka, Y., Yoo, K.H., Lee, J.O., Kawai, T., 2002. Control of electrical conduction in DNA using oxygen hole doping. Appl. Phys. Lett. 80, 1670–1672.

Loesche, M., 1997. Protein monolayers at interfaces. Curr. Opin. Solid State Mater. Sci. 2, 546–556.

Mao, Y., Wei, W., Peng, H., Zhang, J., 2001. Monitoring for adsorption of human serum albumin and bovine serum albumin onto bare and polystyrene modified silver electrodes by quartz crystal impedance analysis. J. Biotechnol. 89, 1–10.

Moulton, S.E., Barisci, J.N., Bath, A., Stella, R., Wallace, G.G., 2003. Investigation of protein adsorption and electrochemical behavior at a gold electrode. J. Colloid Interface Sci. 261, 312–319.

Neff, H., Zong, W., Lima, A.M.N., Borre, M., Holzhüter, G., in press. Optical properties and instrumental performance of thin gold films near the surface plasmon resonance, J. Thin Solid Films.

Norde, W., Giacomelli, C.E., 2000. BSA structural changes during homomolecular exchange between the adsorbed and the dissolved states. J. Biotechnol. 79, 259–268.

Rogers, K.R., Mulchandani, A. (Eds.), 1998. Affinity Biosensors: Techniques and Protocols; and references cited therein; Humana Press, Totowa, New Jersey; ISBN 0-89603-539-5.

Silin, V., Weetall, H., Vanderah, D.J., 1997. SPR studies of the non-specific adsorption kinetics of human IgG and BSA on gold surfaces modified by self assembled monolayers (SAMs). J. Colloid Interface Sci. 185, 94–103.

Thirstrup, C., Zong, W., Borre, M., Neff, H., Pedersen, H.C., Holzhueter, G., 2004. Diffractive optical coupling element for surface plasmon resonance sensors. Sens. Actuators B 100 (3), 298–308.

Vörös, J., 2004. The density and refractive index of adsorbing protein layers. Biophys. J. 87, 553–561.

Wee, K.W., Kang, G.Y., Park, J., Kang, J.Y., Yoon, D.S., Park, J.H., Kim, T.S., 2005. Novel electrical detection of label free disease marker proteins using piezoresistive self-sensing micro-cantilevers. Biosens. Bioelectron. 20, 1932–1938.